World Journal of Condensed Matter Physics, 2026, 16(3), 55-72
https://www.scirp.org/journal/wjcmp
ISSN Online: 2160-6927
ISSN Print: 2160-6919

Theoretical Predictions of Thermodynamic Behavior for Cd-Tl Melts at Different Temperatures

Nabin Kumar Roy[1], Anadi Prasad Singh[2], Rajendra Prasad Chaudhary[3], Jagdhar Mandal[4*], Indu Shekhar Jha[3]

[1]University Department of Chemistry, T.M. Bhagalpur University, Bhagalpur, India
[2]Marwari College, T.M. Bhagalpur University, Bhagalpur, India
[3]Department of Physics, M.M.A.M. Campus, Biratnagar, Nepal
[4]University Department of Physics, T.M. Bhagalpur University, Bhagalpur, India
Email: nabinkrroy@gmail.com, anadisingh888@gmail.com, r.p.chaudhary028@gmail.com, thesaurabhbgp@gmail.com, *jmandal1284@gmail.com, isjha12345@gmail.com

How to cite this paper: Roy, N.K., Singh, A.P., Chaudhary, R.P., Mandal, J. and Jha, I.S. (2026) Theoretical Predictions of Thermodynamic Behavior for Cd-Tl Melts at Different Temperatures. *World Journal of Condensed Matter Physics*, **16**, 55-72.
https://doi.org/10.4236/wjcmp.2026.163004

Received: July 21, 2026
Accepted: August 28, 2026
Published: August 31, 2026

Abstract

The molecular interaction volume model is utilized to analyze the composition dependence of thermodynamic properties like Gibbs excess free energy of mixing, free energy of mixing, activity coefficients, activity, microscopic properties such as concentration fluctuations, short-range order parameter and diffusivity ratio of Cd-Tl melts at 750 K. The required interaction parameters are evaluated by Newton-Raphson method using the observed data of activity coefficients of constituent atoms in the infinite dilute solution region. The computed data for excess free energy of mixing, Gibbs free energy of mixing, activity, activity coefficients and concentration fluctuations exhibit excellent harmony with the analogous experimental data for Cd-Tl melts at 750 K. The observed asymmetries in excess free energy of mixing, free energy of mixing and concentration fluctuations for Cd-Tl melts at 750 K are successfully explained. The short-range order parameter and diffusivity relative to the composition for Cd-Tl melts at 750 K are theoretically predicted. The results illustrate the segregating character of Cd-Tl melts at 750 K. Further, the thermodynamic, microscopic and transport properties of Cd-Tl melts at 650 K, 750 K, 850 K, 950 K and 1050 K are predicted theoretically. The segregating behavior of Cd-Tl melts decreases with the elevation in temperature from 650 - 1050 K.

Keywords

Excess Free Energy of Mixing, Activity Coefficients, Concentration Fluctuations, Short-Range Order Parameter, MIVM Model

1. Introduction

The Cd-Tl and Cd-Tl-based multicomponent alloys like Sn-Cd-Tl, Bi-Cd-Tl, Pb-Cd-Bi-Tl etc., have potential applications in industries, as semiconductors, as ceramic compounds, as microsensor in technological process, etc. [1] [2]. The phase diagram [3] shows that the composition dependence of thermodynamic functions like excess free energy of mixing, G_M^E, free energy of mixing, G_M and enthalpy of mixing, H_M are asymmetric while the entropy of mixing, S_M is symmetric for Cd-Tl melts at 750 K at $x = 0.5$. In the entire composition region $x = 0.1$ to 0.9, G_M^E and H_M have positive values at each composition. The activity of both the components *i.e.* a_{Cd} and a_{Tl} illustrates the positive departures from the ideal mixing behaviour. Therefore, Cd-Tl system at 750 K in molten state has a segregating character [4].

The thermodynamic properties and wide range of applications indicate the importance of the Cd-Tl melts for the researchers. Nevertheless, there is scarcity of data related to the study of thermophysical properties of Cd-Tl in the literature. Earlier, some attempts have been made to explore the thermodynamic properties like H_M and activity of the components Cd and Tl, and phase diagram by the optimization process on using CALPHAD approach [5] and G_M, concentration fluctuations, $S_{cc}(0)$, diffusivity, D and viscosity of Cd-Tl melts at 750 K by quasi-lattice theory [6]. Despite these, Cd-Tl melts at 750 K still requires further investigation.

In present work, MIVM model is utilized for the analysis of G_M^E, G_M, activity coefficients, γ_υ, activity, $S_{cc}(0)$, short-range order parameter, α_1 (SRO), excess stability function, E^{XS} and transport property like diffusivity ratio, $\frac{D_M}{D_{id}}$ of Cd-Tl melts at 650 K, 750 K, 850 K, 950 K and 1050 K. The MIVM model [7] is a fluid-based model based on the statistical thermodynamics. It is necessary to point out that MIVM model is successfully employed for the analysis of the thermodynamic properties of several binary alloys (Zn-Bi, Al-Ga, Ni-Pd, Al-In, Zn-Cd, etc.) and multi-component alloys (Au-Sn-Bi, Au-Sn-Zn, Zn-In-Sn, Al-Sn-Zn, Zn-Cu-Sn-In, etc.) [8]-[15].

2. Formalism

2.1. Thermodynamic Properties Like Excess Free Energy of Mixing, G_M^E, Free Energy of Mixing, G_M, Activity Coefficient, γ_υ and Activity, $a_\upsilon(\upsilon = i, j)$ of Binary Molten Alloys

MIVM model is established by Tao [7] which is a fluid-based model and deduced from statistical thermodynamics, the fundamental notion of non-random interchange of liquid molecules and fluid-phase equilibria. For a binary melt $i-j$, the molecular excess free energy of mixing is expressed as [7]

$$\frac{G_M^E}{RT} = x_i \ln\left(\frac{V_{mi}}{x_i V_{mi} + x_j V_{mj} A_{ji}}\right) + x_j \ln\left(\frac{V_{mj}}{x_j V_{mj} + x_i V_{mi} A_{ij}}\right) - \frac{x_i x_j}{2}\left(\frac{Z_i A_{ji} \ln A_{ji}}{x_i + x_j A_{ji}} + \frac{Z_j A_{ij} \ln A_{ij}}{x_j + x_i A_{ij}}\right) \quad (1)$$

where, the compositions of the element i and j represented by x_i and x_j, A_{ij} and A_{ji} refer to pair-potential energy interaction parameters, respectively and the first coordination numbers of the constituents i and j are respectively Z_i and Z_j. The pair potential energy interaction parameters may be expressed as [7]

$$A_{ji} = \exp\left[-\frac{\varepsilon_{ji} - \varepsilon_{ii}}{kT}\right] \text{ and } A_{ij} = \exp\left[-\frac{\varepsilon_{ij} - \varepsilon_{jj}}{kT}\right] \tag{2}$$

where, ε_{ii}, ε_{jj} and ε_{ji} stand for potential energies for the pairs $i-i$, $j-j$ and $i-j$ respectively, temperature is represented by T and k represents Boltzmann constant. It is noted that $\varepsilon_{ij} = \varepsilon_{ji}$.

The partial molar energy and excess molar free energy are related as

$$G_M^{\bar{E}} = RT\ln\gamma_\upsilon = G_M^E + \delta\left(\frac{\partial G_M^E}{\partial x_i}\right)_{T,P,x[i,N]} - \sum_{j=1}^{N}\left(\frac{\partial G_M^E}{\partial x_i}\right)_{T,P,x[j,N]} \tag{3}$$

where, $\gamma_\upsilon(\upsilon = i, j)$ represents the activity coefficient of binary melts.

It is noted that Equation (3) follows the condition that for $i \neq N$, $\delta = 1$; and $i = N$, $\delta = 0$. Again, the variables x_j and x_N determined from $x[i,N]$ with $x_N = 1 - \sum_{j=1}^{N-1} x_j$. Hence, the activity coefficients of components i and j of a binary melt are respectively, represented by

$$\begin{aligned}\ln\gamma_i = {} & \ln\left(\frac{V_{mi}}{x_i V_{mi} + x_j V_{mj} A_{ji}}\right) + x_j\left(\frac{V_{mj}A_{ji}}{x_i V_{mi} + x_j V_{mj} A_{ji}} - \frac{V_{mi}A_{ji}}{x_j V_{mj} + x_i V_{mi} A_{ij}}\right) \\ & - \frac{x_j^2}{2}\left(\frac{Z_i A_{ji}^2 \ln A_{ji}}{\left(x_i + x_j A_{ji}\right)^2} + \frac{Z_j A_{ij} \ln A_{ji}}{\left(x_j + x_i A_{ij}\right)^2}\right)\end{aligned} \tag{4}$$

and

$$\begin{aligned}\ln\gamma_j = {} & \ln\left(\frac{V_{mj}}{x_j V_{mj} + x_i V_{mi} A_{ij}}\right) - x_i\left(\frac{V_{mj}A_{ji}}{x_i V_{mi} + x_j V_{mj} A_{ji}} - \frac{V_{mi}A_{ij}}{x_j V_{mj} + x_i V_{mi} A_{ij}}\right) \\ & - \frac{x_i^2}{2}\left(\frac{Z_j A_{ij}^2 \ln A_{ij}}{\left(x_j + x_i A_{ij}\right)^2} + \frac{Z_i A_{ji} \ln A_{ji}}{\left(x_i + x_j A_{ji}\right)^2}\right)\end{aligned} \tag{5}$$

For the component i, the first co-ordination number is determined by the following relation [7]

$$Z_i = \frac{4\sqrt{2\pi}}{3}\left(\frac{r_{mi}^3 - r_{oi}^3}{r_{mi} - r_{oi}}\right)\rho_i r_{mi} \exp\left(\frac{\Delta H_{mi}\left(T_{mi} - T\right)}{Z_C R T_{mi}}\right) \tag{6}$$

where, T_{mi} represents the melting temperature in kelvin, ΔH_{mi}, the enthalpy at melting temperature, $\rho_i = N_i V_i = \dfrac{0.6022}{V_{mi}}$ represents the molecular number density, r_{mi} and r_{oi} are initial value and first peak value for radial distribution function of metal i in molten state near T_{mi}, R stands for molar gas constant and Z_C represents the co-ordination number for closed packed structure which is usually taken to be 12. The radial distances may be represented by

$$r_{oi} = 0.918 d_{\mathrm{cov},i} \quad \text{and} \quad r_{mi} = \sigma_i \tag{7}$$

where, d_{cov} represents atomic covalent diameter and σ_i the atomic diameter.

In infinite dilute solution region, such as x_i or $x_j \to 0$, the activity coefficients of the constituents i and j may be represented by

$$\ln \gamma_i^{\infty} = 1 - \ln\left(\frac{V_{mj}A_{ji}}{V_{mi}}\right) - \frac{V_{mi}A_{ji}}{V_{mj}} - \frac{1}{2}\left(Z_i \ln A_{ji} + Z_j A_{ij} \ln A_{ij}\right) \tag{8}$$

and

$$\ln \gamma_j^{\infty} = 1 - \ln\left(\frac{V_{mi}A_{ij}}{V_{mj}}\right) - \frac{V_{mj}A_{ji}}{V_{mi}} - \frac{1}{2}\left(Z_j \ln A_{ij} + Z_i A_{ji} \ln A_{ji}\right) \tag{9}$$

The activity and activity coefficients for the constituents of the binary melts may be expressed as [4]

$$a_i = \gamma_i x_i \tag{10a}$$

$$a_j = \gamma_j x_j \tag{10b}$$

2.2. Microscopic Functions Like Concentration Fluctuations, $S_{cc}(0)$ and SRO, α_1 of a Binary Molten Alloy

The $S_{cc}(0)$ and α_1 are found to be very important microscopic parameters to explore the interatomic interactions in a liquid system. If $S_{cc}(0) < S_{cc}^{id}(0)$ then the system is ordered *i.e.* dissimilar ($i-j$) atoms or molecules coupled together as the closest neighbors. Similarly, $S_{cc}(0) > S_{cc}^{id}(0)$ describes the segregating character of the binary melt and like (*i.e.* $i-i$ or $j-j$) atoms or molecules link together as the closest neighbors [4].

The G_M and $S_{cc}(0)$ are related as [4] [16]

$$S_{cc}(0) = RT\left(\frac{\partial^2 G_M}{\partial x_i^2}\right)^{-1}_{T,P,N} = RT\left(\frac{\partial^2 G_M}{\partial x_j^2}\right)^{-1}_{T,P,N} \tag{11}$$

where,

$$G_M = G_M^E + G_M^{id} \tag{12}$$

$$\Rightarrow G_M = G_M^E + RT\left[x_i \ln x_i + x_j \ln x_j\right] \tag{13}$$

Using Equations (1) and (13) in (11), one can obtain

$$S_{cc}(0) = \frac{x_i x_j}{1 + x_i x_j f\left(x_i x_j\right)} \tag{14}$$

where,

$$\begin{aligned} f\left(x_i, x_j\right) = {} & \frac{V_{mj}A_{ji} - V_{mi}}{x_i V_{mi} + x_j V_{mj} A_{ji}} + \frac{V_{mi}A_{ij} - V_{mj}}{x_j V_{mj} + x_i V_{mi} A_{ij}} + \frac{V_{mj}A_{ji}\left(V_{mj}A_{ji} - V_{mi}\right)}{\left(x_i V_{mi} + x_j V_{mj} A_{ji}\right)^2} \\ & + \frac{V_{mi}A_{ij}\left(V_{mi}A_{ij} - V_{mj}\right)}{\left(x_j V_{mj} + x_i V_{mi} A_{ij}\right)^2} + \left[\frac{Z_i A_{ji}^2 \ln A_{ji}}{\left(x_i + x_j A_{ji}\right)^3} + \frac{Z_j A_{ij}^2 \ln A_{ij}}{\left(x_j + x_i A_{ij}\right)^3}\right] \end{aligned} \tag{15}$$

For an ideal mixing, $G_M = G_M^{id}$ hence Equations (14) and (15) yield

$$S_{cc}^{id}(0) = x_i x_j \tag{16}$$

Again, the activity and $S_{cc}(0)$ are related as

$$S_{cc}(0) = a_i x_j \left(\frac{\partial a_i}{\partial x_i}\right)^{-1} = a_j x_i \left(\frac{\partial a_j}{\partial x_j}\right)^{-1} \tag{17}$$

The $S_{cc}(0)$ determined from Equation (17) on utilizing the experimental data of activity is considered as the experimental data [4] [16] [17].

The SRO, α_1 initiated by Warren-Cowley [18] [19] is related to $S_{cc}(0)$ as [4] [20]

$$\alpha_1 = \frac{S-1}{S(Z-1)+1} \quad \text{with} \quad S = \frac{S_{cc}(0)}{S_{cc}^{id}(0)} \tag{18}$$

where, Z refers to the coordination number in first neighbor shell.

Equation (18) exhibits that α_1 = positive for segregating system, α_1 = negative for ordered system and $\alpha_1 = 0$ for ideal mixture.

2.3. Excess Stability Function, E^{XS} and Diffusivity, D of a Binary Molten Alloy

The excess stability function, E^{XS} initiated by Darken [21] [22] may be expressed as

$$\frac{E^{XS}}{RT} = S_{cc}(0))^{-1} - \left(S_{cc}^{id}(0)\right)^{-1} \tag{19}$$

Obviously, E^{XS} = positive for ordering alloy, E^{XS} = negative for segregating alloy and $E^{XS} = 0$ for ideal alloy depending upon the conditions that $S_{cc}(0) < S_{cc}^{id}(0)$, $S_{cc}(0) > S_{cc}^{id}(0)$, and $S_{cc}(0) = S_{cc}^{id}(0)$ respectively.

The transport property, such as diffusivity is very useful to describe the mixing behavior of a binary solution at the microscopic level. For a binary liquid system, the diffusivity ratio is expressed as [4] [23]

$$\frac{D_M}{D_{id}} = \frac{S_{cc}^{id}(0)}{S_{cc}(0)} \tag{20}$$

where, D_M and D_{id} represent the mutual diffusion coefficient of the system and intrinsic diffusion coefficient of ideal system respectively. Now, D_{id} is represented by

$$D_{id} = x_i D_j + x_j D_i \tag{21}$$

where, D_i and D_j are self-diffusion coefficients of pure elements i and j respectively.

Equation (20) illustrates that $D_M / D_{id} > 1$ for ordered system, $D_M / D_{id} < 1$ for segregating system and $D_M / D_{id} = 1$ for ideal system.

3. Results and Discussions

3.1. Excess Free Energy of Mixing, G_M^E, Free Energy of Mixing, G_M, Activity Coefficient, γ_υ and Activity, $a_\upsilon(\upsilon = i, j)$ of Cd-Tl Melts at 750 K

The analytical equations for G_M^E, G_M, γ_μ and $a_\mu(\mu = i, j)$ are employed to assess the thermodynamic properties of Cd-Tl melts at 750 K. The necessary parameters of pure Cd and Tl are presented in **Table 1** [24]. The coordination numbers Z_i and Z_j of the constituents of the alloy are determined from Equation (6) which are presented in **Table 2**. The parameters A_{ji} and A_{ij} are evaluated on solving Equations (8) and (9) simultaneously by Newton-Rapson method using the values of infinite dilute activity coefficients *i.e.* γ_i^∞ (1.932) and γ_j^∞ (3.826) [3]. The evaluated values of A_{ji} and A_{ij} are 0.7107 and 0.8815 respectively. The approximated values of A_{ji} and A_{ij} are slightly altered in order to achieve a good harmony between the theory and experiment [3] for G_M^E of Cd-Tl melts at 750 K. The reasonable values of A_{ji} and A_{ij} *i.e.* 0.7120 and 1.0990 respectively, are also incorporated in **Table 2**.

Table 1. Input parameters for the pure metals [24].

Metal, i	ΔH_{mi} (KJ/mole)	σ_i (×10^{-8} cm)	r_{oi} (×10^{-8} cm)	V_{mi} (cm^3/mole)
Cd	6.40	3.00	2.54	14.0 [1 + 1.6 × 10^{-4} (T-594)]
Tl	4.31	3.22	2.74	18.0 [1 + 1.15 × 10^{-4} (T-575.65)]

Table 2. Values of A_{ij}, A_{ji}, Z_i and Z_j for the constituents of Cd-Tl melts at required temperature.

$i-j$	T(K)	A_{ij}	A_{ji}	Z_i	Z_j
Cd-Tl	650	0.6757	1.1151	9.86	9.53
	750	0.7120	1.0990	9.71	9.42
	850	0.7410	1.0869	9.56	9.32
	950	0.7648	1.0774	9.41	9.22
	1050	0.7846	1.0698	9.27	9.12

The values of G_M^E/RT calculated from Equation (1) as a function of Cd for Cd-Tl alloys at 750 K show excellent agreement with the corresponding experimental values [3] as presented in **Figure 1**. In composition region, $x_{Cd} = 0.1$ to 0.9, the value of G_M^E is positive at each concentration. The computed and experimental [3] values of G_M^E/RT are in excellent harmony with maximum values at $x_{Cd} = 0.6$ *i.e.* 0.2478 (Theory) and 0.2504 (Experiment). The RMS error is found to be 0.00533% on employing Equation (22). Hence, the present theoretical investigation successfully reveals the symmetry in G_M^E/RT and segregating nature of Cd-Tl melts at 750 K.

$$\text{RMS Error} = \sqrt{\frac{\sum_{i=1}^{n}\left(x_i - y_i\right)^2}{n}} \tag{22}$$

where,

x_i = theoretical (calculated) values;

y_i = experimental values;

n = no. of data points.

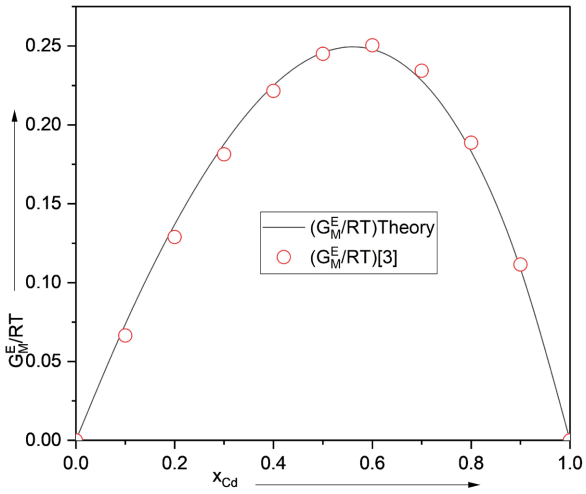

Figure 1. G_M^E/RT vs x_{Cd} for Cd-Tl melts at 750 K.

Equation (13) is used to compute the values of G_M/RT for Cd-Tl melts at 750 K which are illustrated in **Figure 2** along with experimental values [3]. A well agreement is seen. In the whole composition region, $x_{Cd} = 0.1$ to 0.9, G_M/RT is negative with minimum values at x_{Cd} = 0.4 *i.e.* $G_M/RT\left(\min^m\right) = -0.4481$ (Theory) and −0.4518 (Experiment). The RMS error computed from Equation (22) is found to be 0.00542%. Thus, the symmetry in G_M/RT is successfully described by MIVM model.

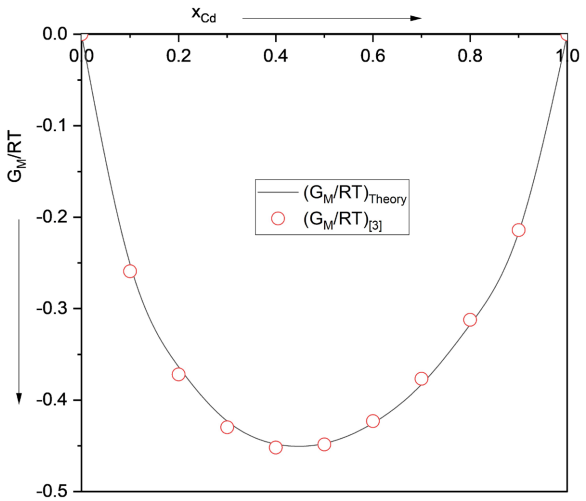

Figure 2. G_M/RT vs x_{Cd} for Cd-Tl melts at 750 K.

The activity coefficients γ_{Cd} and γ_{Tl} are evaluated from Equations (4) and (5) respectively in terms of the concentration of Cd. The theoretical and experimental [3] data of γ_{Cd} and γ_{Tl} are in excellent agreement as shown in **Figure 3**. The RMS errors for γ_{Cd} and γ_{Tl} computed from Equation (22) are found to be 0.029441% and 0.022264% respectively.

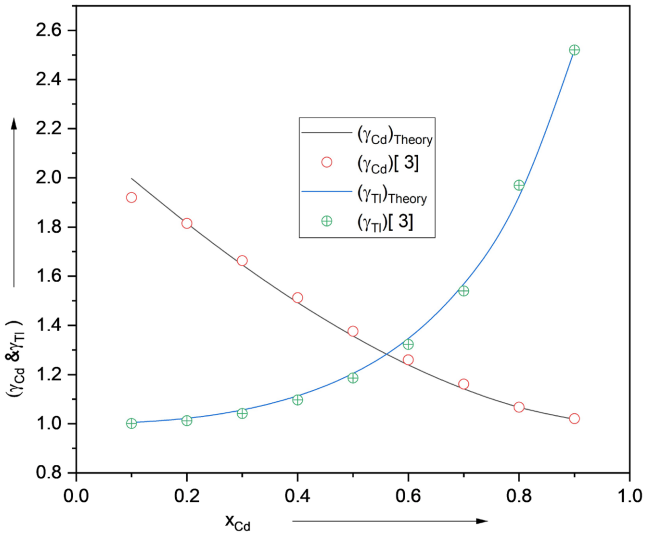

Figure 3. (γ_{Cd} & γ_{Tl}) vs x_{Cd} for Cd-Tl melts at 750 K.

The theoretical data of γ_{Cd} and γ_{Tl} are used to calculate the concentration dependence of a_{Cd} and a_{Tl} respectively from Equations (10a) and (10b) for Cd-Tl melts at 750 K, which are presented in **Figure 4**.

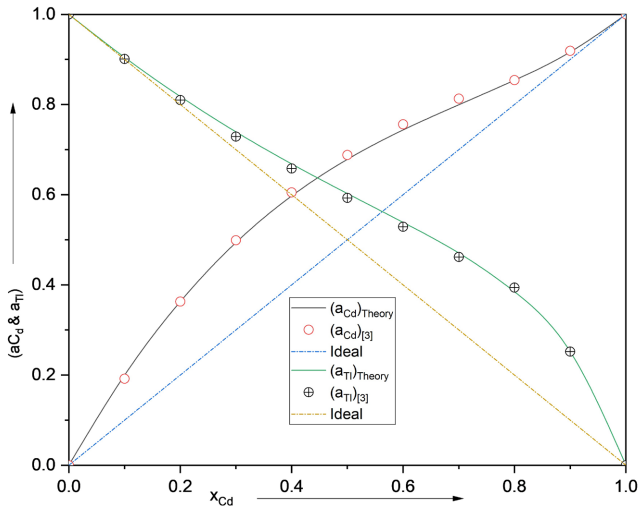

Figure 4. (a_{Cd} & a_{Tl}) vs x_{Cd} for Cd-Tl melts at 750 K.

A well concord is noticed between theory and experiment [3] with RMS errors for a_{Cd} and a_{Tl} computed from Equation (22) are found to be 0.008040% and 0.008330% respectively. The positive departures of a_{Cd} and a_{Tl} from ideal

behavior refer to the segregating character of Cd-Tl melts at 750 K. It should be pointed out that the activity is a fortunate thermodynamic function which can be directly measured from the experiment. Therefore, the well harmony between theoretical and experimental data for a_{Cd} and a_{Tl} validates the reasonable values of A_{ji} and A_{ij}.

3.2. Microscopic Properties Like $S_{cc}(0)$, α_1, E^{XS} and D_M/D_{id} of Cd-Tl Molten Melts at 750 K

Equations (14) and (15) are employed to compute the concentration dependence of $S_{cc}(0)$ for Cd-Tl melts at 750 K. The theoretical data of $S_{cc}(0)$ are incorporated in **Figure 5** along with $S_{cc}^{id}(0)$ and experimental values [3].

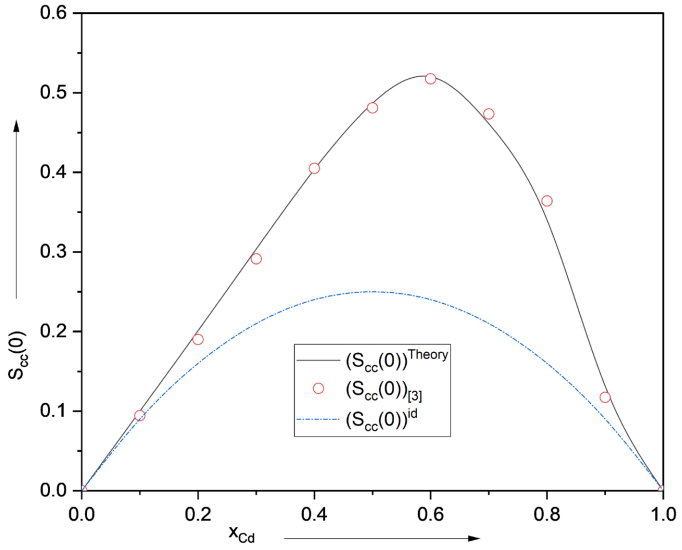

Figure 5. $S_{cc}(0)$ vs x_{Cd} for Cd-Tl melts at 750 K.

A well uniformity is noticed between the theory and experiment having the RMS error of 0.0118705% which is computed from Equation (22). It is observed that $S_{cc}(0) > S_{cc}^{id}(0)$ in the composition region, $0.1 \le x_{Cd} < 0.95$ and $S_{cc}(0)$ exhibits ideal behavior of Cd-Tl melts at 750 K in the regions $0 \le x_{Cd} \le 0.1$ and $0.95 \le x_{Cd} < 1.0$. The maximum values of $S_{cc}(0)$ are at $x_{Cd} = 0.60$ *i.e.* $S_{cc}(0)(\max^{m}) = 0.520$ (Theory) and 0.518 (Experiment). Hence, the present investigation reveals that Cd-Tl melt at 750 K possesses segregating character in the region $0.1 \le x_{Cd} < 0.95$.

Equation (18) is employed to achieve the concentration dependent values of α_1 for Cd-Tl melts at 750 K on using $Z = 10$. The theoretical data of α_1 in terms of the concentration of Cd are presented in **Figure 6**. In the full range of composition *i.e.* $x_{Cd} = 0.1$ to 0.9, α_1 is positive at each composition and having maximum value of 0.0576 at $x_{Cd} = 0.7$, which reveals the segregating behavior of Cd-Tl melts at 750 K [25].

The concentration dependence of E^{XS}/RT for Cd-Tl alloys at 750 K

computed from Equation (19) is illustrated in Figure 7. Obviously, E^{XS}/RT is negative at each composition of Cd in the concentration region $x_{Cd} = 0.10$ to 0.90 for Cd-Tl melts at 750 K. This exhibits the segregating nature of Cd-Tl melts at 750 K [22] [26].

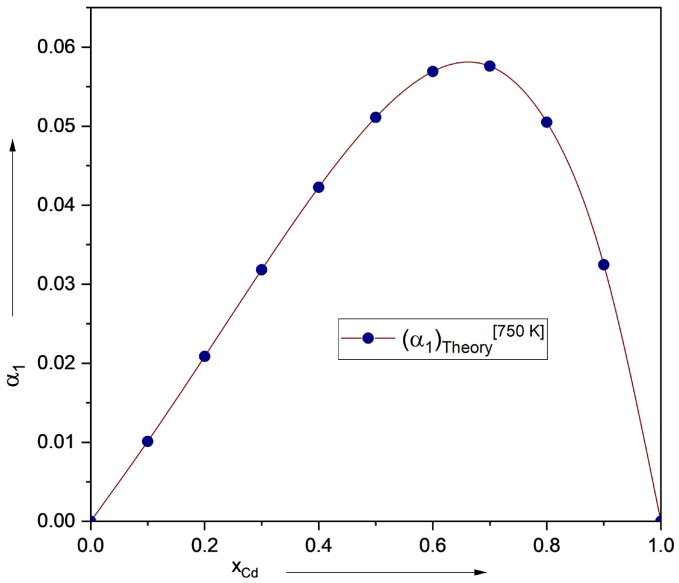

Figure 6. α_1 vs x_{Cd} for Cd-Tl melts at 750 K.

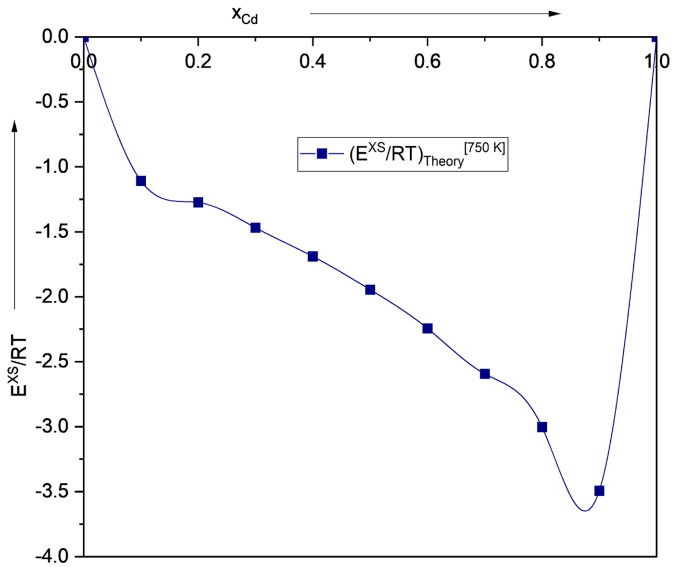

Figure 7. E^{XS}/RT vs x_{Cd} for Cd-Tl melts at 750 K.

The diffusivity ratio, D_M/D_{id} as a function of the composition of Cd for Cd-Tl melts at 750 K is calculated from Equation (20) and the theoretical data of D_M/D_{id} are depicted in Figure 8. It is noticed that the diffusivity ratio, D_M/D_{id} has minimum value of 0.4554 at 750 K at $x_{Cd} = 0.7$. This confirms the segregation in Cd-Tl melts at 750 K [4].

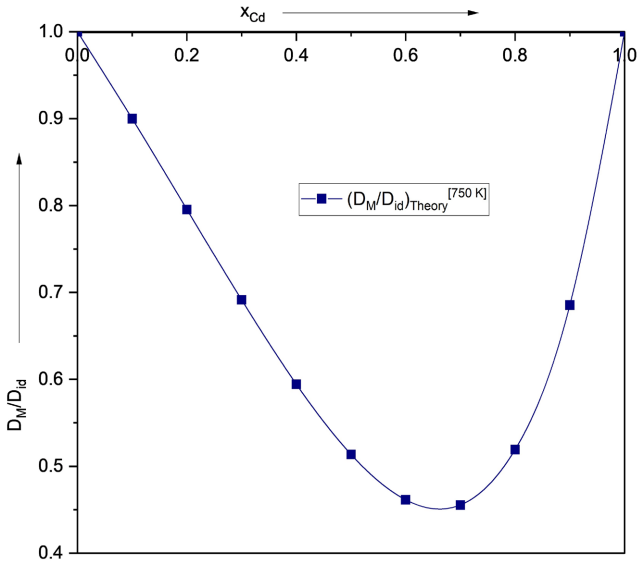

Figure 8. D_M/D_{id} vs x_{Cd} for Cd-Tl melts at 750 K.

3.3. G_M^E, G_M, a_{Fe}, a_{Mn}, $S_{cc}(0)$, E^{XS}, α_1 and D_M/D_{id} of Cd-Tl Melts at Different Temperatures

For the theoretical analysis of the mixing behavior of Cd-Tl melts at different temperatures, the needed input parameters are presented in Table 1 and Table 2. The values of A_{ji} and A_{ij} at desired temperature, T K are determined via the following equations [7].

$$-\frac{\varepsilon_{ji}-\varepsilon_{ii}}{kT}=T\ln A_{ji}(T)=T_0\ln A_{ji}(T_0)$$

$$A_{ji}(T)=\exp\left(\frac{T_0\ln A_{ji}(T_0)}{T}\right) \tag{22}$$

and

$$-\frac{\varepsilon_{ij}-\varepsilon_{jj}}{kT}=T\ln A_{ij}(T)=T_0\ln A_{ij}(T_0)$$

$$A_{ij}=\exp\left(\frac{T_0\ln A_{ij}(T_0)}{T}\right) \tag{23}$$

where, T_0 = 750 K.

The computed data of G_M^E/RT and G_M/RT for Cd-Tl melts assessed via Equations (1) and (13) at 650 K, 750 K, 850 K, 950 K and 1050 K are presented in Figure 9 and Figure 10 respectively. Figure 9 illustrates that the segregating nature of Cd-Tl melts degrades when temperature is upgraded from 650 K to 1050 K. The maximum values of G_M^E/RT are 0.2767 (at 650 K), 0.2478 (at 750 K), 0.2234 (at 850 K) all $x_{Cd}=0.6$ while $G_M^E/RT(\max^m)=0.2033$ (at 950 K) and 0.1863 (at 1050 K) both at $x_{Cd}=0.5$. Thus, Cd-Tl melts exhibit asymmetric behavior at 650 K, 750 K and 850 K, and symmetric character at 950 K and 1050 K relative to the composition of Cd. Again, it is noticeable from Figure 10 that the

negative values of G_M/RT for Cd-Tl melts increase due to rise in temperature from 650 K to 1050 K. The values of G_M/RT are minimum at $x_{Cd}=0.4$ for temperatures 650 K and 750 K *i.e.* −0.4256 and −0.4481, respectively while G_M/RT shows minima at $x_{Cd}=0.5$ for temperatures 850 K, 950 K and 1050 K *i.e.* −0.4703, −0.4899 and −0.5068 respectively in terms of x_{Cd}. Thus, Cd-Tl melts indicate asymmetry at 650 K and 750 K and symmetry at 850 K, 950 K and 1050 K with respect to x_{Cd}.

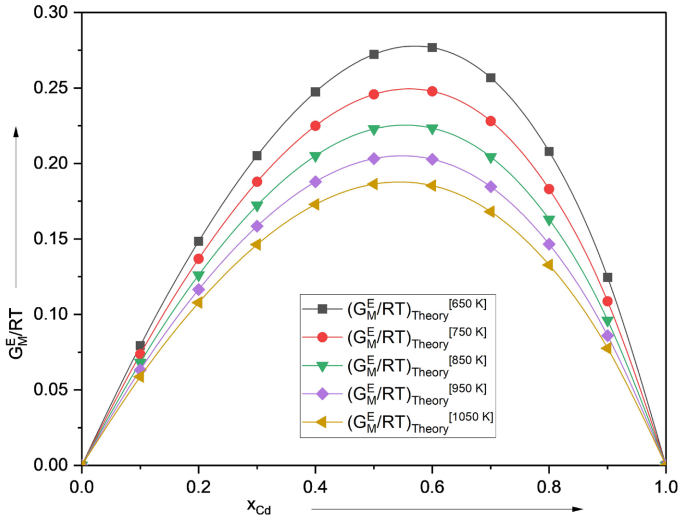

Figure 9. G^E_M/RT vs x_{Cd} for Cd-Tl melts at 650 K, 750 K, 850 K, 950 K & 1050 K.

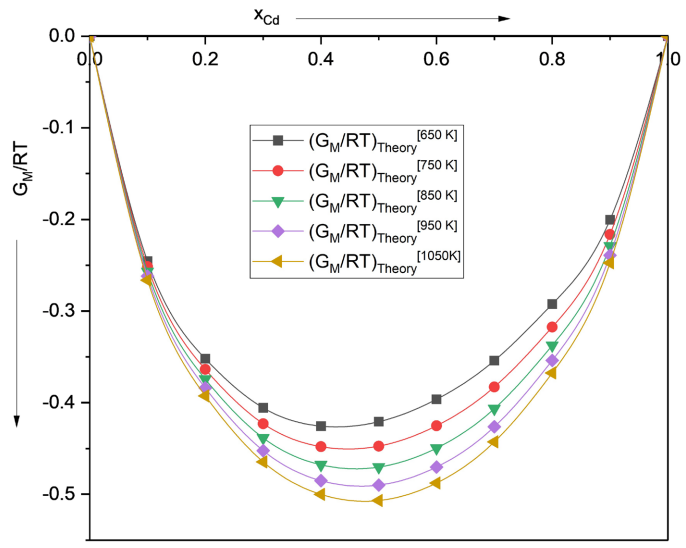

Figure 10. G_M/RT vs x_{Cd} for Cd-Tl melts at 650 K, 750 K, 850 K, 950 K & 1050 K.

The thermodynamic activities of Cd and Tl *i.e.* a_{Cd} and a_{Tl} are computed from Equations (10a) and (10b) respectively on applying the theoretical data of γ_{Cd} and γ_{Tl} determined from Equations (4) and (5) for Cd-Tl melts at 650 K, 750 K, 850 K, 950 K and 1050 K relative to x_{Cd}. The theoretical results for a_{Cd}

and a_{Tl} at the temperatures ranging from 650 K to 1050 K are shown in Figure 11. The results reveal the decrease in segregation for rise in temperature from 650 K to 1050 K for Cd-Tl melts. However, the decrease in the segregation is weak in the temperature region 650 - 1050 K.

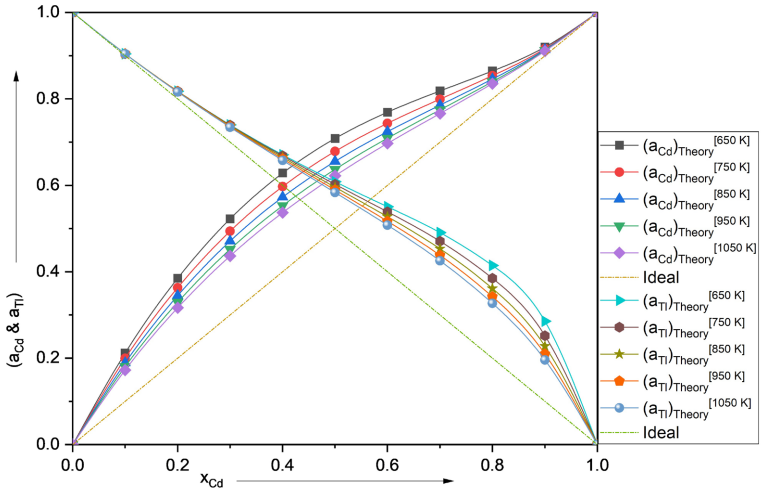

Figure 11. (a_{Cd} & a_{Tl}) vs x_{Cd} for Cd-Tl melts at 650 K, 750 K, 850 K, 950 K & 1050 K.

The temperature dependence of $S_{cc}(0)$ for Cd-Tl melts at 650 K, 750 K, 850 K, 950 K and 1050 K relative to composition Cd is presented in Figure 12. For the calculation of $S_{cc}(0)$, Equations (14) and (15) are applied. The $S_{cc}(0)$ - x_{Cd} isotherms indicate the degradation in segregating character of Cd-Tl melts for the rise in temperature from 650 K to 1050 K. The peak value of $S_{cc}(0)$ is noticed at $x_{Cd} = 0.6$ *i.e.* 0.618, 0.520, 0.466 and 0.427 respectively at 650 K, 750 K, 850 K, 950 K while a minor shift in peak value of $S_{cc}(0)$ is observed at 1050 K *i.e.* $S_{cc}(0) = 0.405$ at $x_{Cd} = 0.53$.

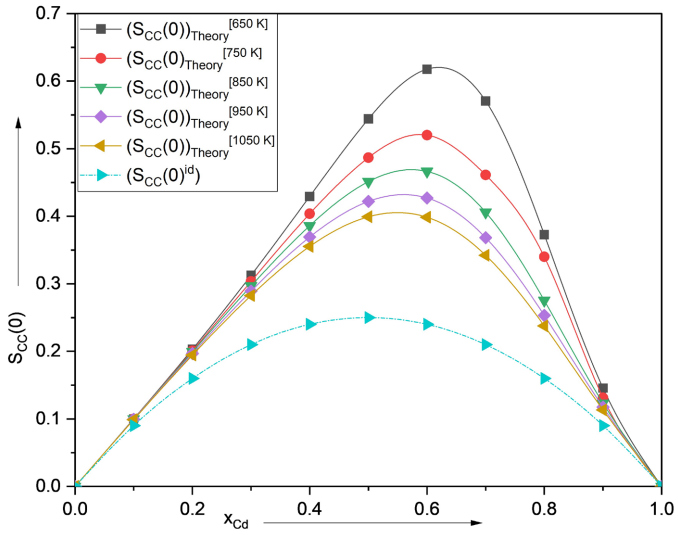

Figure 12. $S_{cc}(0)$ vs x_{Cd} for Cd-Tl melts at 650 K, 750 K, 850 K, 950 K & 1050 K.

The α_1 - x_{Cd} isotherms for Cd-Tl melts are depicted in **Figure 13**. For this, the theoretical data of α_1 are computed with the help of Equation (18) at temperatures 650 - 1050 K. Obviously, the segregation in Cd-Tl melts goes on decreasing for the rise in temperature from 650 K to 1050 K. Again, the magnitude of α_1 is small which illustrates that Cd-Tl melts is a weakly segregating system [4] [26] in the temperature range 650 - 1050 K.

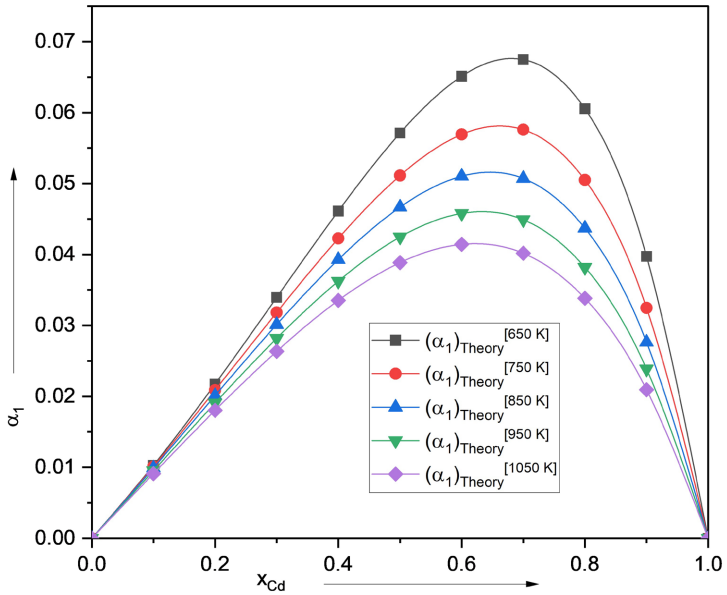

Figure 13. α_1 vs x_{Cd} for Cd-Tl melts at 650 K, 750 K, 850 K, 950 K & 1050 K.

The excess stability function of several binary alloys at a certain temperature has been discussed earlier [27] [28]. Nonetheless, the limited data is available regarding the theoretical exploration of E^{XS} at different temperatures [22] [26], [29] on employing the optimization procedure. In present study, MIVM model is applied to explore the stability of Cd-Tl melts at various temperatures.

The variation of E^{XS}/RT with respect to composition of Cd at 650 K, 750 K, 850 K, 950 K and 1050 K for Cd-Tl melts determined via Equation (19) is presented in **Figure 14**. Obviously, E^{XS}/RT exhibits negative value at each composition in the region $x_{Cd} = 0.10$ to 0.90 at each temperature under consideration. Again, the negative values of E^{XS}/RT declines with the upgradation in temperature from 650 K to 1050 K. This is a sign of decrease in the segregation of Cd-Tl melts [22] [26] from 650 K to 1050 K.

The D_M/D_{id} relative to the concentration of Cd for Cd-Tl melts at 650 K, 750 K, 850 K, 950 K and 1050 K are computed using Equation (20) and the theoretical data are depicted in **Figure 15**. It is noticed that $D_M/D_{id} < 1$ at the temperatures under consideration which confirms the segregating character of Cd-Tl melts. Again, D_M/D_{id} has minimum values at $x_{Cd} = 0.7$ *i.e.* 0.3679 and 0.4554 respectively for 650 K and 750 K and again, has minimum values at $x_{Cd} = 0.6$ *i.e.* 0.5145, 0.5621 and 0.6022 for 850 K, 950 K and 1050 K respectively. This indicates

lowering of segregating character of Cd-Tl melts at the undertaken temperatures.

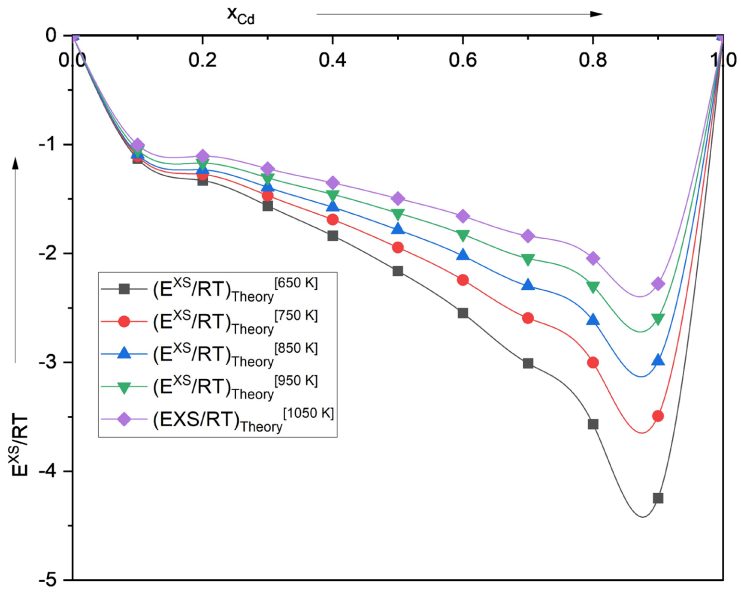

Figure 14. E^{XS}/RT vs x_{Cd} for Cd-Tl melts at 650 K, 750 K, 850 K, 950 K & 1050 K.

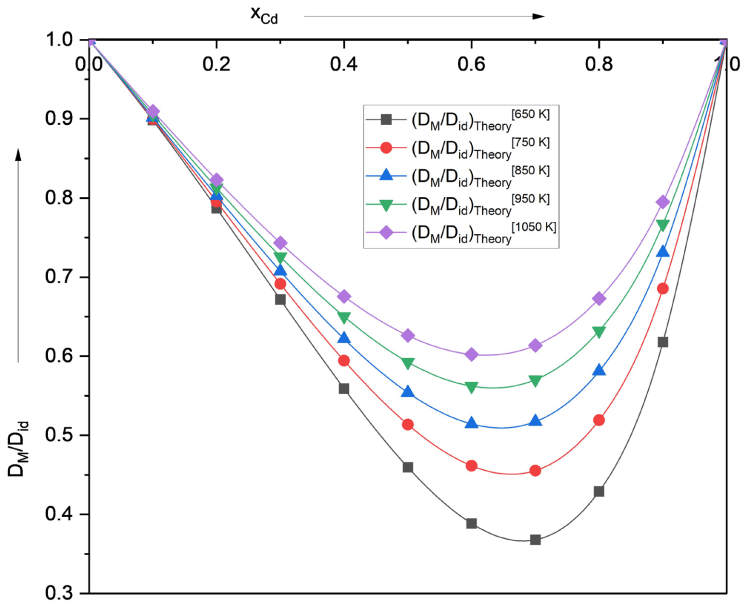

Figure 15. D_M/D_{id} vs x_{Cd} for Cd-Tl melts at 650 K, 750 K, 850 K, 950 K & 1050 K.

4. Conclusions

In present work, the concentration dependent properties such as G_M^E, G_M activity coefficient, activity, $S_{cc}(0)$, α_1, E^{XS} and D_M/D_{id} for Cd-Tl melts at 750 K have been successfully explored. The results exhibit the segregating nature of Cd-Tl melts at 750 K. The asymmetries in G_M^E, G_M and $S_{cc}(0)$ for Cd-Tl melts at 750 K are successfully explained. Again, MIVM model is employed for the theoretical predictions of G_M^E, G_M activity, $S_{cc}(0)$, α_1, E^{XS} and

D_M/D_{id} for Cd-Tl melts at 650 K, 750 K, 850 K, 950 K and 1050 K. The results indicate that the segregating character of Cd-Tl melts degrades when temperature rises from 650 K to 1050 K. Further, Cd-Tl melt is a feebly segregating alloy in the temperature range 650 - 1050 K.

Therefore, MIVM model is a relevant and reliable model to explore the thermodynamic behavior of segregating alloys at different temperatures.

Author Contributions

Conceptualization, I. S. Jha and J. Mandal; methodology, N. K. Roy; validation, I. S. Jha, J. Mandal and R. P. Chaudhary; formal analysis; R. P. Chaudhary; investigation, A. P. Singh; writing original draft preparation, A. P. Singh; writing-review and editing, N. K. Roy; visualization, I. S. Jha; supervision, J. Mandal. All authors have read and agreed to published version of the manuscript.

Conflicts of Interest

The authors declare no conflicts of interest regarding the publication of this paper.

References

[1] Dinsdale, A.T. (1991) SGTE Data for Pure Elements. *Calphad*, **15**, 317-425. https://doi.org/10.1016/0364-5916(91)90030-n

[2] Pelton, A.D. (1988) The Cd-Na (Cadmium-Sodium) System. *Bulletin of Alloy Phase Diagrams*, **9**, 41-46. https://doi.org/10.1007/bf02877458

[3] Hultgren, R., Desai, P.D., Hawkins, D.T., Gleiser, M. and Kelley, K.K. (1973) Selected Values of the Thermodynamic Properties of Binary Alloys. Metal Park (Ohio), ASM.

[4] Singh, R.N. and Sommer, F. (1997) Segregation and Immiscibility in Liquid Binary Alloys. *Reports on Progress in Physics*, **60**, 57-150. https://doi.org/10.1088/0034-4885/60/1/003

[5] Liu, Y.J., Yu, D. and Ge, Y. (2009) Thermodynamic Optimization of the Cd-Na and Cd-Tl Binary Systems. *Journal of Alloys and Compounds*, **473**, 60-64. https://doi.org/10.1016/j.jallcom.2008.05.106

[6] Awe, O.E. (2018) Thermodynamic Investigation of Thermophysical Properties of Thallium-Based Liquid Alloys. *Physics and Chemistry of Liquids*, **57**, 296-310. https://doi.org/10.1080/00319104.2018.1443453

[7] Tao, D.P. (2000) A New Model of Thermodynamics of Liquid Mixtures and Its Application to Liquid Alloys. *Thermochimica Acta*, **363**, 105-113. https://doi.org/10.1016/s0040-6031(00)00603-1

[8] Ding, G.H., Liang, L.M., Meng, P., Wang, L., Wang, Y.X., Wang, Y.J., *et al.* (2019) Application of the Molecular Interaction Volume Model to the Assessment of Thermodynamic Properties of Liquid Zn-Bi Alloys. *Metallic Materials*, **57**, 55-60. https://doi.org/10.4149/km_2019_1_55

[9] Yang, H.W., Tao, D.P. and Zhou, Z.H. (2008) Prediction of the Mixing Enthalpies of Binary Liquid Alloys by Molecular Interaction Volume Model. *Acta Metallurgica Sinica* (*English Letters*), **21**, 336-340. https://doi.org/10.1016/s1006-7191(08)60056-3.

[10] Liang, L.M., Ding, G.H., Wang, Y.X. and Liu, Y. (2021) Thermodynamic Properties of Liquid Zn-Cd Alloys Investigated by the Molecular Interaction Volume Model.

Physics and Chemistry of Liquids, **59**, 706-715.
https://doi.org/10.1080/00319104.2020.1808655

[11] Awe, O.E. and Oshakuade, O.M. (2017) Theoretical Prediction of Thermodynamic Activities of Liquid Au-Sn-X (X=Bi, Sb, Zn) Solder Systems. *Physica B: Condensed Matter*, **507**, 84-94. https://doi.org/10.1016/j.physb.2016.11.035

[12] Roy, N.K., Vrind, N., Sahu, R.K., Mandal, J. and Jha, I.S. (2025) Prediction of the Alloying Behaviour of Ni-Pd Melts by Molecular Interaction Volume Model. *IOP Conference Series: Materials Science and Engineering*, **1334**, Article 012005. https://doi.org/10.1088/1757-899x/1334/1/012005

[13] Sah, S.K., Jha, I.S. and Koirala, I. (2023) Theoretical Examination of Some Thermodynamic Properties in In-Bi-Sn Liquid Alloy and Its Sub-Binary Systems. *Journal of Electronic Materials*, **52**, 6350-6359. https://doi.org/10.1007/s11664-023-10571-y

[14] Odusote, Y.A., Popoola, A.I., Adedayo, K.D. and Ogunjo, S.T. (2017) Thermodynamic Properties of Al in Ternary Lead-Free Solder Al-Sn-Zn Alloys. *Materials Science-Poland*, **35**, 583-593. https://doi.org/10.1515/msp-2017-0080

[15] Sah, S.K., Jha, I.S. and Koirala, I. (2024) Thermodynamic Activity in Zn-Cu-Sn-In Liquid Solder Alloys: A Comprehensive Analysis Using the Molecular Interaction Volume Model. *Welding International*, **38**, 265-276. https://doi.org/10.1080/09507116.2024.2325151

[16] Bhatia, A.B. and Thornton, D.E. (1970) Structural Aspects of the Electrical Resistivity of Binary Alloys. *Physical Review B*, **2**, 3004-3012. https://doi.org/10.1103/physrevb.2.3004

[17] Bhatia, A.B. and Hargrove, W.H. (1974) Concentration Fluctuations and Thermodynamic Properties of Some Compound Forming Binary Molten Systems. *Physical Review B*, **10**, 3186-3196. https://doi.org/10.1103/physrevb.10.3186

[18] Warren, B.E. (1969) X-Ray Diffraction. Addison-Wesley Publishing Company.

[19] Cowley, J.M. (1950) An Approximate Theory of Order in Alloys. *Physical Review*, **77**, 669-675. https://doi.org/10.1103/physrev.77.669

[20] Singh, R.N. (1987) Short-Range Order and Concentration Fluctuations in Binary Molten Alloys. *Canadian Journal of Physics*, **65**, 309-325. https://doi.org/10.1139/p87-038

[21] Darken, L.S. (1967) Thermodynamics of Binary Metallic Solutions. *Transactions of the Metallurgical Society of AIME*, **239**, 80-89.

[22] Singh, A.P., Chaudhary, R.P., Kumari, R., Jha, I.S. and Mandal, J. (2022) Stability of NaK Liquid Alloys at Different Temperatures. *Materials Today: Proceedings*, **66**, 2251-2258. https://doi.org/10.1016/j.matpr.2022.06.097

[23] Darken, L.S. (1948) Diffusion, Mobility and Their Interrelation through Free Energy in Binary Metallic Systems. *Transactions of AIME*, **175**, 184-201.

[24] Iida, T. and Guthrie, R.I.L. (1988) The Physical Properties of Liquid Metals. Oxford University Press.

[25] Chaudhary, R.P., Mandal, J. and Jha, I.S. (2022) Concentration Dependence of the Bulk and Surface Properties of Liquid AlZn Alloys at 1000 K. *Materials Today: Proceedings*, **59**, 397-404. https://doi.org/10.1016/j.matpr.2021.11.358

[26] Singh, A.P., Chaudhary, R.P., Hussain, M.M., Mandal, J. and Jha, I.S. (2025) Theoretical Study of the Stability of CdSn Liquid Alloy at Different Temperatures. *Diffusion Foundations and Materials Applications*, **37**, 37-51. https://doi.org/10.4028/p-efgqf5

[27] Jha, I.S., Singh, R.N., Srivastava, P.L. and Mitra, N.R. (1990) Stability of HgNa and

HgK Liquid Alloys. *Philosophical Magazine B*, **61**, 15-24. https://doi.org/10.1080/13642819008208649

[28] Abodunrin, O.W. and Ajayi, A.A. (2022) Calculation of Excess Stability Functions of Four Binary Alloys. *Jordan Journal of Physics*, **14**, 193-200.

[29] Shrestha, G.K., Singh, B.K., Jha, I.S., Singh, B.P. and Adhikari, D. (2017) Optimization Method for the Study of the Properties of Al-Sn Binary Liquid Alloys. *Physica B: Condensed Matter*, **514**, 1-7. https://doi.org/10.1016/j.physb.2017.03.005